

CHAPTER III

RESULTS AND DISCUSSION

3.1 Synthesis of P3HT

The was obtained P3HT as sticky black solid like rubber up to 82% yield. The Head-to-Tail (HT) percentage was determined to be 80% higher than those reported in literature [16] (74% yield and 68% HT) using the same method. From $^1\text{H-NMR}$ spectrum, (Figure A-1, Appendix A), P3HT showed characteristic hexyl signals of the $-\text{CH}_3$ at 0.91 ppm, $-(\text{CH}_2)_4$ at 0.91-1.8 ppm. The aromatic protons of thiophene rings from four environments (section 1.2.3) appeared as four resonances at δ 6.9-7.0 ppm (Figure 3.1). The α -protons from two other different regioregularities (HT and HH) were observed at δ 2.74 and 2.50 ppm, respectively.

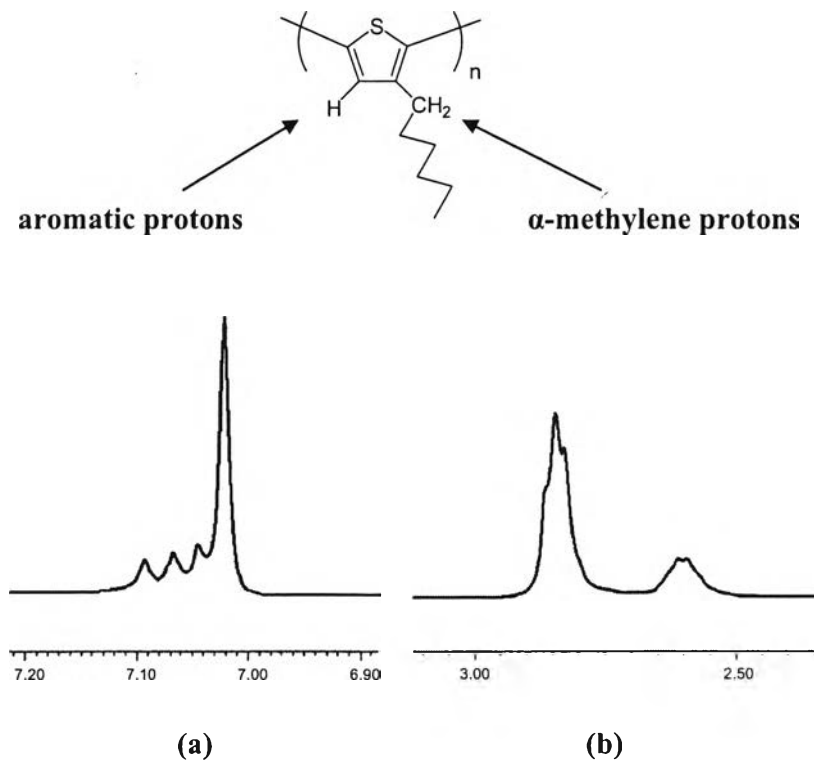


Figure 3.1 Part of $^1\text{H-NMR}$ spectrum of P3HT showing (a) aromatic protons and (b) α -methylene protons

P3HT showed a dominant signal at 6.90 ppm and three weaker yet well defined signals at 6.93, 6.95, and 6.98 ppm. The δ 6.90 ppm resonance arised from rings involved in the HT-HT linkages whilst those at 6.93, 6.95, and 6.98 ppm account for HT-HH, TT-HT, and TT-HT linkages, respectively. [11,12] The results are in accord with the literature.

In IR spectrum, P3HT showed the expected peaks as assigned in **Table 3.1**, (**Figure A-2**, Appendix A) which were also corresponded well to that reported in literature [38]. From UV-visible spectrum in CHCl_3 , P3HT has λ_{max} at 441 nm (**Figure A-3**, Appendix A).

Table 3.1 Assignments of the IR spectrum of poly(3-hexylthiophene)

Assignments	Wave number (cm^{-1})
aromatic C-H stretching	3050
aliphatic C-H stretching	2953, 2921, 2852
ring stretching	1513, 1458
methyl bending	1369
aromatic C-H out-of-plane	820
methylene rocking	723

3.2 The fractionation of P3HT

As-synthesized P3HT has been fractionated into five fractions differing in their solubility and molecular weight. The low molecular weight fraction contains shorter chain polymer that is well soluble in acetone. The higher molecular weight polymer has poorer solubility and requires solvent in the compromised range of polarity such as CHCl_3 .

Table 3.2 Macromolecular parameters of P3HT fractions from consecutive extractions

fraction	wt%	M_n	M_w	P_i	D_n
acetone	13.5	1,543	1,872	1.22	9
hexane	27.0	6,456	8,950	1.38	38
CH ₂ Cl ₂	30.6	26,588	45,761	1.72	160
10%CHCl ₃ in CH ₂ Cl ₂	26.0	53,255	82,216	1.54	320
CHCl ₃	2.9	67,013	95,725	1.43	403

Table 3.2 shows macromolecular parameters, derived from gel permeation chromatographic measurements. The average molecular weights and the polydispersity of all fractions except acetone fraction were higher than that was reported by Trznadel and coworkers, [46b] in which their P3HT was synthesized from Grignard reaction that is known to be of higher selectivity than the oxidative coupling.

The UV-visible spectra of the separated fractions of P3HT both in the solution and solid-state (**Figure 3.2** and **Figure 3.3**) showed gradual bathochromic shifts of λ_{max} with the increase of the average molecular weight of the fractions. These shifts were more pronounced in the solid films. The solvatochromic effect observed in this case for poly(3-hexylthiophene) is amplified from 3 nm for the acetone fraction to 64 nm for the CHCl₃ one.

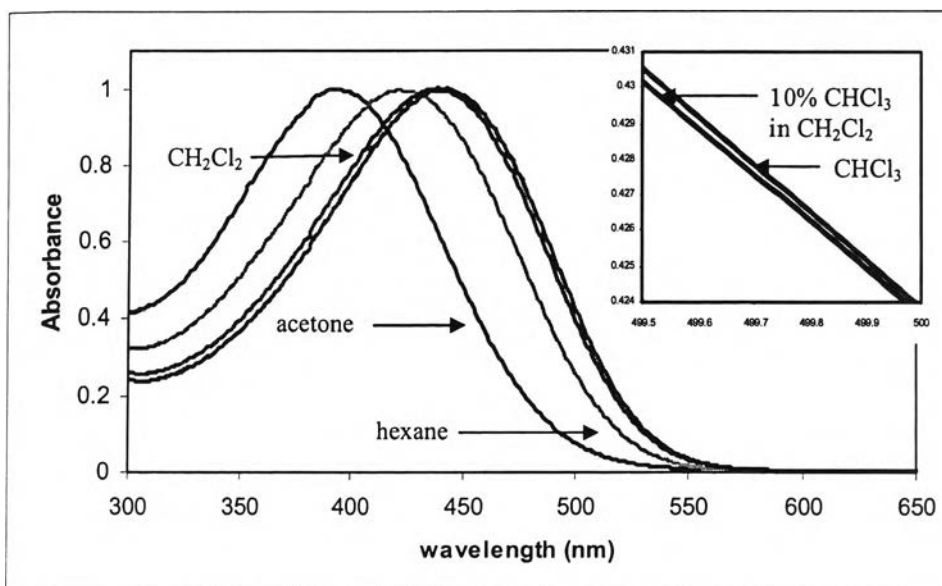


Figure 3.2 UV-visible spectra of the fractions of poly(3-hexylthiophene)(P3HT) from consecutive extractions.

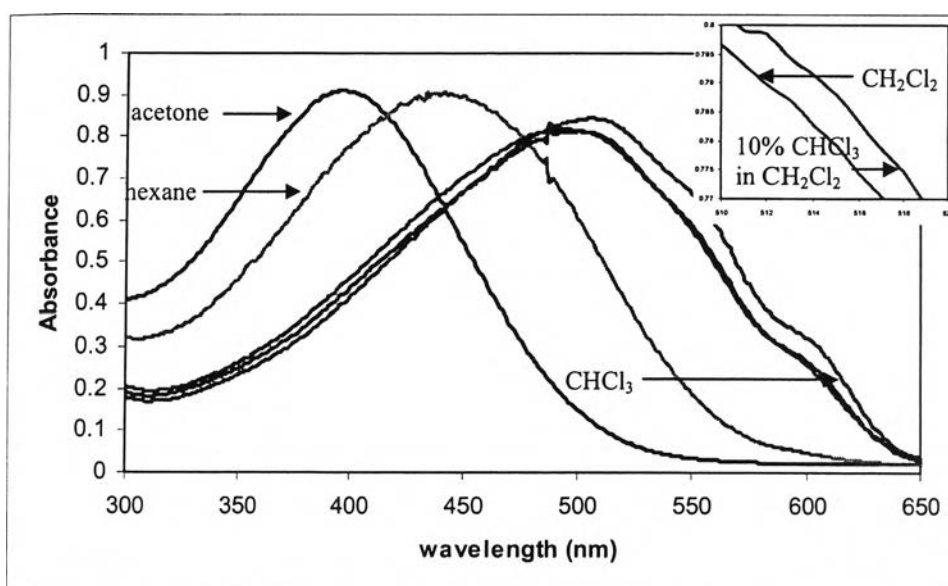


Figure 3.3 UV-visible spectra of solid film cast from evaporation of the fractions of poly(3-hexylthiophene)(P3HT) from consecutive extractions.

In comparison with the solution, the further bathochromic shift in the solid state was in accordance with previous report which was described as intrachain coil-to-rod conformational change from solution to the solid state, resulting in extended delocalization (Figure 3.4) [48].

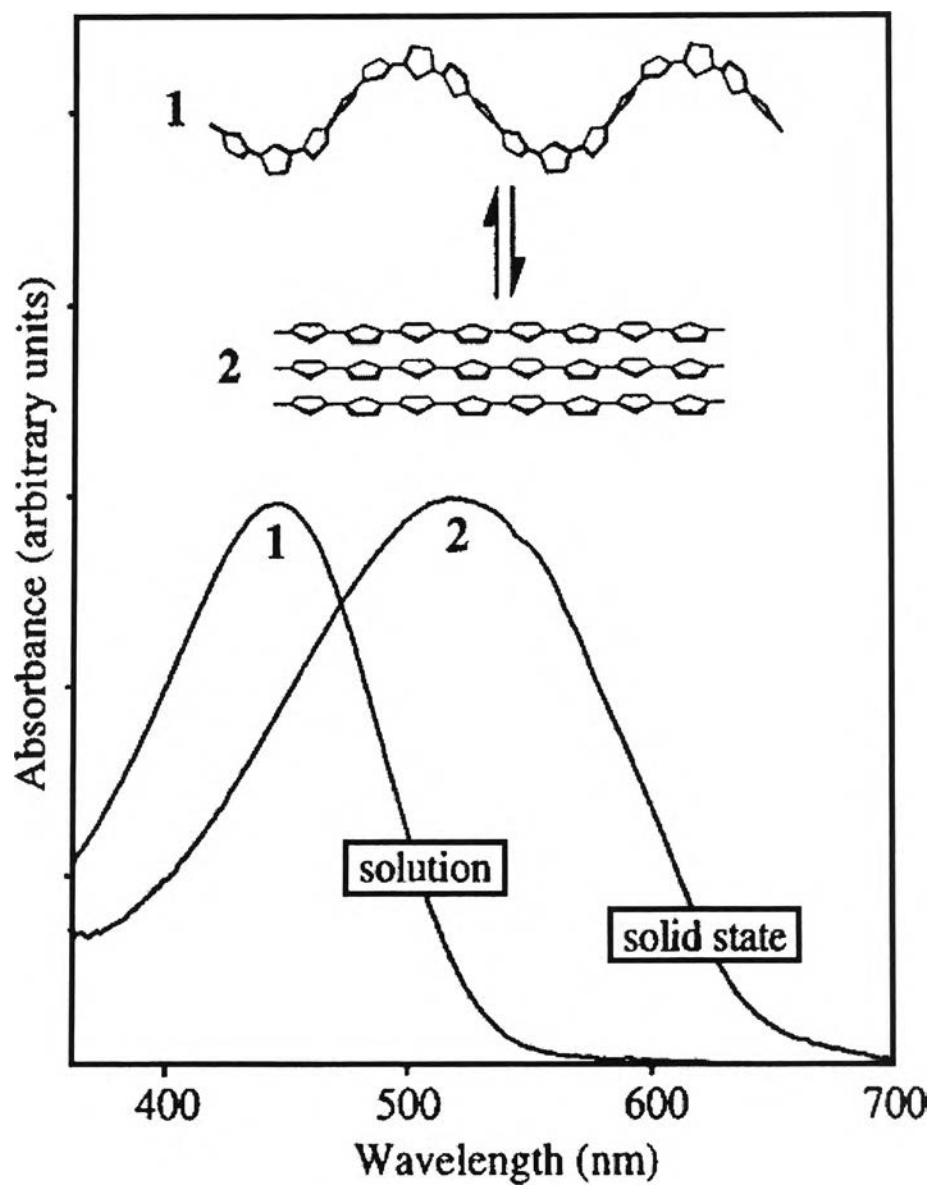


Figure 3.4 CHCl_3 solution and solid-state UV-visible spectra of polythiophene derivatives.

The ^1H NMR spectra of the five fractions are different at α -methylene protons of hexyl group and aromatic proton shown in **Figure 3.5**.

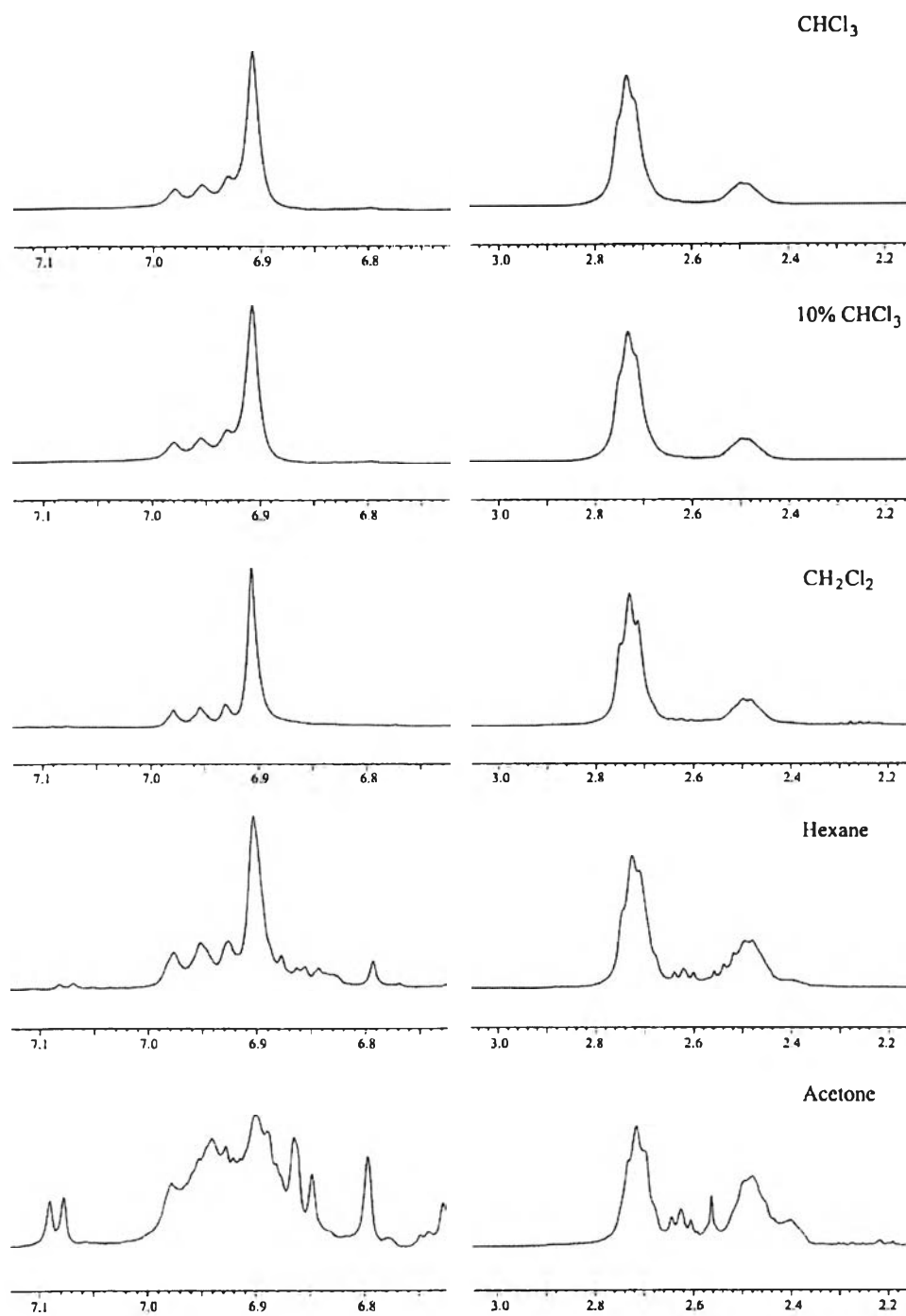


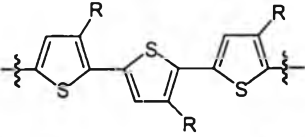
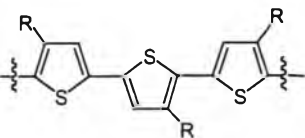
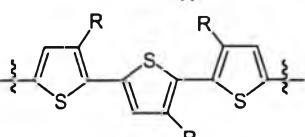
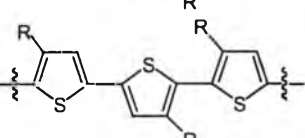
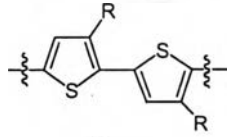
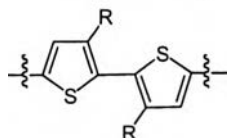
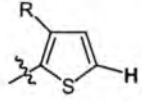
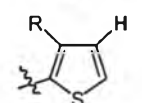
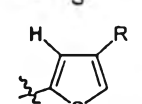
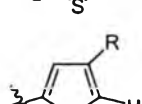
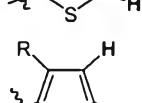
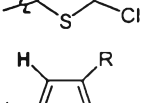
Figure 3.5 ^1H NMR spectra of poly(3-hexylthiophene) fractions differing in their average molecular weight.

From **Figure 3.5**, the noise signals observed (mostly founded in acetone fraction) and aromatic correspond to the protons in the terminal thiophene rings (end groups) (presented in **Table 3.3**). Their intensity quickly decreased in the fractions with higher average molecular weights because of lower the number of protons from the terminal thiophene rings. At the α -methylene groups of the alkyl substituents, the ratios of the signal at 2.74 to the signal at 2.50 ppm increase with the fractions with higher average molecular weights, indicating the increase of % HT in these.

From the combined results of UV-visible spectra and $^1\text{H-NMR}$ spectra, λ_{max} and %HT were found to increase with the average molecular weight and level off at the CH_2Cl_2 fraction, indicating that the structures of high molecular weight polymers are quite similar (**Figure 3.6** and **3.7**). The oxidative polymerization is known to be initiated through radicals, which gives a nonselective reaction. Initially, the two molecules of monomers react with each other at 2-position, where the electro density is higher than 5-position due to the electron donating alkyl groups. The reactions between growing polymers produce both HT and HH linkages. But the long chain polymer favors the formation of HT linkage because of lower steric hindrance between coupling units. Therefore, the longer polymer chain (higher molecular weight) have higher %HT, hence higher λ_{max} .

From UV-visible spectra, λ_{max} usually corresponds to the main chromophore of a molecule that most absorbs the incoming light. The position and intensity of the absorbance at λ_{max} are generally the characteristic information that can be correlated to some properties of the molecule. In macromolecules or polymers, however, the information at λ_{max} may only partly reflect their important characters. This is especially significant for conjugated polymers, when the absorptions at various regions would correspond to many conjugated systems that all variedly contribute to the macroscopic properties of the polymer.

Table 3.3 ^1H NMR chemical shifts of aromatic and α -methylene protons in triads and end groups of poly(3-hexylthiophene)

	Protons	δ (ppm)	
		aromatic	α -methylene
Triads		6.90	-
		6.92	-
		6.95	-
		6.98	-
Diads		2.72	-
		2.98	-
Terminal Protons		7.09	-
		7.08	-
		6.87	2.60-2.70
		6.85	2.60-2.70
		6.80	2.35-2.60
		6.78	2.35-2.60

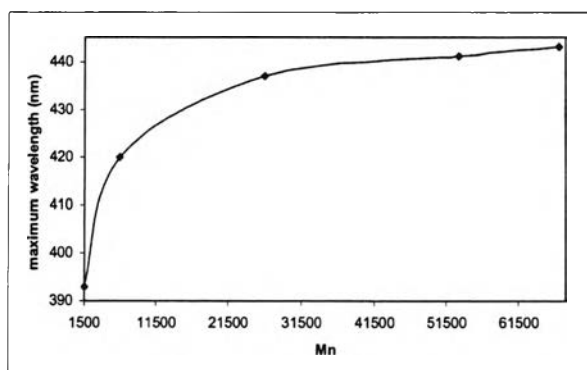


Figure 3.6 λ_{\max} of poly(3-hexylthiophene) fractions ranged by their average molecular weight (see also **Table D-1**, Appendix D)

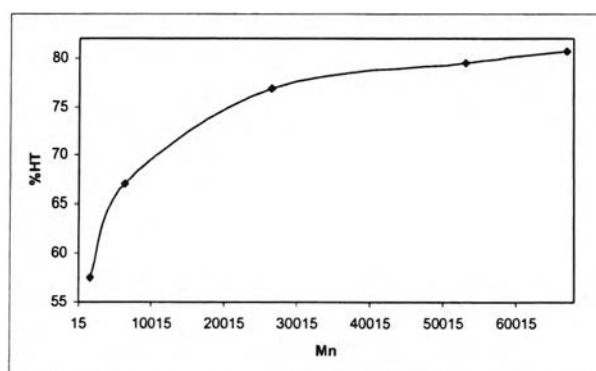


Figure 3.7 %HT of poly(3-hexylthiophene) fractions ranged by their average molecular weights (the calculations and the results were shown in **Table C-1**, Appendix C, and **Table D-2**, Appendix D, respectively)

Absorption Conjugation index value (AC-index) has been proposed as a “weighted integrative” absorption at a range of wavelengths. The higher λ values were “weighted” to be more important than that of lower values because of their presumed correspondence to the more conjugated systems. The sum of these weighted absorbances normalized over the sum of the unweighted ones are the AC-index value: high AC-index value would reflect the high effective conjugation length within the polymer chain which could, in turn, correlate to high conductive properties. The equation for the calculation of AC-index value is shown below (example for the AC-index value calculation was shown in appendix C):

$$\text{AC-index (from } \lambda_1 \text{ to } \lambda_{n+1}) = \frac{\sum \lambda_i A_i}{\sum A_i}$$

when λ = wavelength (nm)

A_i = absorbance at λ_i

$i = 1, 2, 3, \dots, n + 1$

In this study, AC-index values were calculated from the 300-700 nm region of the UV-visible spectra. A plot of this AC-index values against the average molecular weight of P3HT fractions is shown in **Figure 3.8**. It was found that the AC-index curve shows similar trend as the former plots using λ_{max} and %HT parameters (**Figures 3.6 and 3.7**), indicating that the AC-index values could be another parameter that would eventually link to many important structural information, as what we expect from λ_{max} .

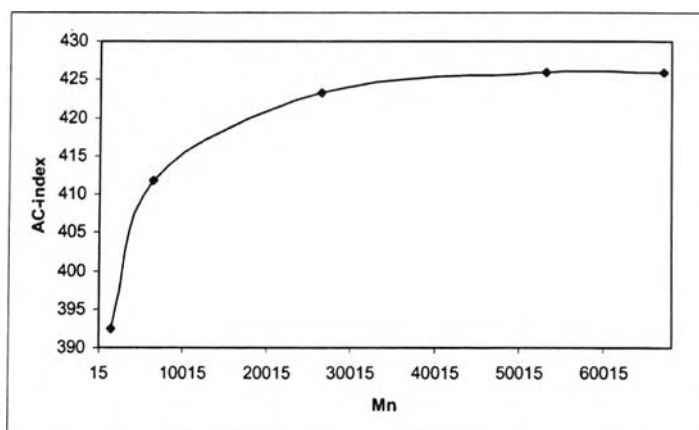


Figure 3.8 AC-index values of poly(3-hexylthiophene) fractions ranged by their average molecular weight (**Table D-3**, Appendix D).

3.3 The doping of P3HT

3.3.1 Doping with trifluoroacetic acid (TFA)

The addition of TFA into P3HT solution, made the orange solution of P3HT from orange to dark brown solution and even darker at higher doping level. The polymer solution gave higher absorbance at higher wavelength when increased the volume of TFA added, possibly because of the formation of polarons (**Figure 3.9**).



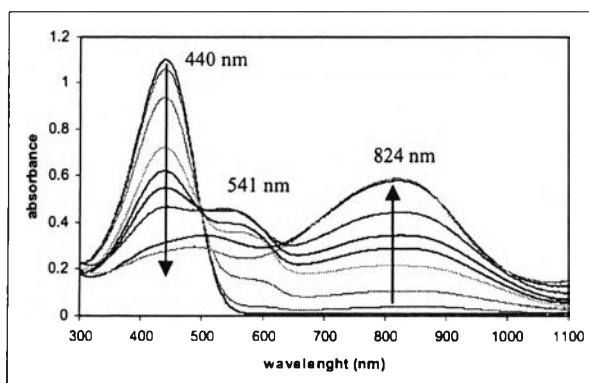


Figure 3.9 UV-visible spectra of P3HT doped with trifluoroacetic acid (TFA) at different equivalent.

From **Figure 3.9**, There are significant changes at 3 wavelength regions (440, 541, and 824 nm). The plots between the absorbances of these three wavelength and equivalents of added TFA are shown in **Figure 3.10**.

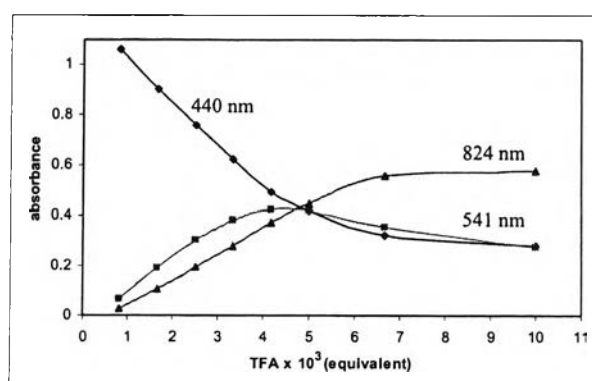


Figure 3.10 Absorbance of P3HT doped with trifluoroacetic acid (TFA):
 (◆) 440 nm; (■) 541 nm; (▲) 824 nm (**Table D-4**, Appendix D).

From **Figure 3.9**, the absorbance curve at 440 nm is an absorption of undoped P3HT (**Figure A-3**, Appendix A). This absorbance decreases when the amount of TFA increase. Because after putting TFA into undoped P3HT, protonation of P3HT occurred and made the polarons of P3HT which gain longer effective conjugation length. This effect result in the decreasing of absorbance at 440 nm while the amount of TFA slowly increased. The absorbance at 541 and 824 nm are absorptions of the intermediate of doped P3HT and doped P3HT polaron respectively. Both curves (541 and 824 nm) showed the upward trend along with TFA amount until the TFA amount

reaches to 6.67×10^3 equivalents. All of the curves go into the equilibrium as shown in **Figure 3.10**.

The UV-visible spectra of the doping P3HT with TFA at various equivalents were recalculated into AC-index values (300-1000 nm) and plotted in **Figure 3.11**.

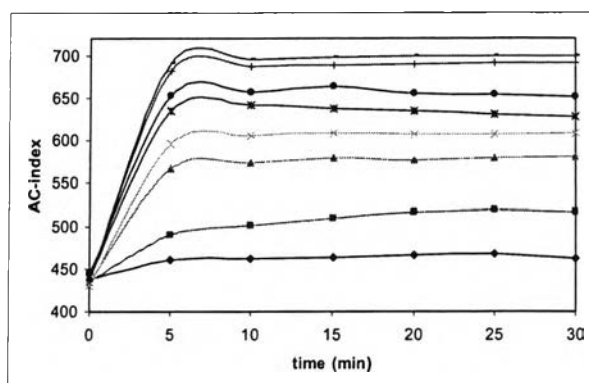


Figure 3.11 AC-index curves of P3HT doped with trifluoroacetic acid (TFA) at various equivalents (**Table D-5**, Appendix D)

The plot of AC-index values of all equivalence of TFA added after 30 min in the **Figure 3.11** was shown in **Figure 3.12**.

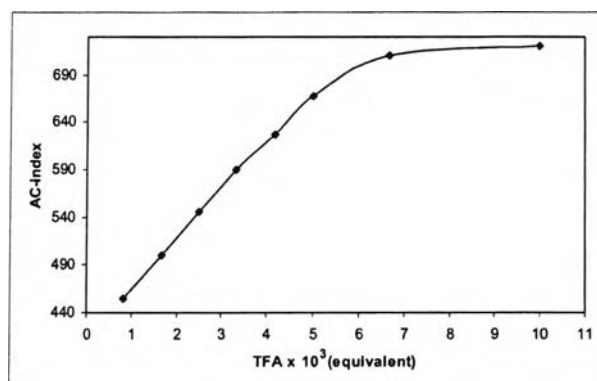


Figure 3.12 AC-index curves of P3HT doped with trifluoroacetic acid (TFA) at 30 min (**Table D-5**, Appendix D)

The resulting curve is quite similar to the absorbance curve at 824 nm (**Figure 3.10**). The AC-index curve shows that the more TFA added, the more polaron or bipolaron are formed, together with the increase in effective conjugation length of P3HT. This demonstrated the applicability of using the AC-index values determine

the doping level of polymer. Which is more sensitive than the absorbance of polaron especially at low if dope polymer in low doping level.

3.3.2 Doping with methanesulfonic acid (MSA)

MSA, however, cannot completely dissolve in CHCl_3 at the same doping level as TFA in the previous experiment. As a result, smaller amounts of MSA (0.33 and 0.5×10^3 equivalents) for doping were used to maintain homogeneity. We also found that this incomplete solvation reflected in the longer time needed for doping process to reach equilibrium. From the plot of AC-index values against time after the addition of acid doping, MSA doping still showed gradual increase of AC-index even after one hour, especially when used at higher amount (**Figure 3.13**).

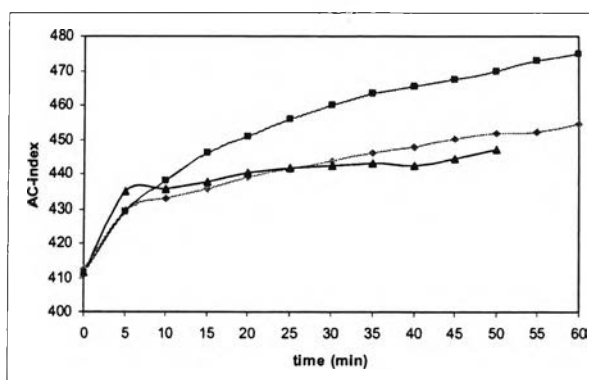


Figure 3.13 AC-index curves of P3HT doped with acid: (◇) MSA 0.33×10^3 equivalents; (■) MSA 0.5×10^3 equivalents; (▲) TFA 0.83×10^3 equivalents (**Table D-6**, Appendix D).

In comparison to the AC-index values from the doping with TFA, lesser amount of MSA gave higher AC-index values due to its stronger acidity. Changing the solvent to CH_3CN to increase solubility of MSA surprisingly gave very low AC-index values. Although these low values are in accord with TFA doping in CH_3CN . We guess that CH_3CN may decrease the doping level of polymer because the acid preferred protonating the polar solvent to the polymer.

3.3.3 Doping with acetic acid

It was envisaged that, the weaker acetic acid which is soluble in CHCl_3 should be conveniently used as a doping agent. Upon doping P3HT with acetic acid, however, no significant change was observed in the UV-visible spectrum even when a large amount of acetic acid was used ($10, 20, \text{ and } 30 \times 10^3$ equivalents) (Figure 3.14). The slight decrease of the λ_{max} at 440 nm is assumed to be due to the dilution from the addition of the acid.

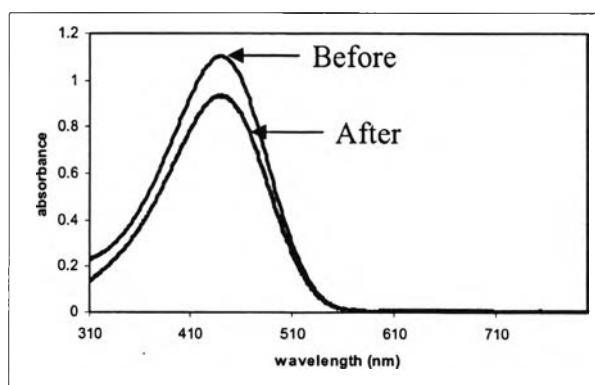


Figure 3.14 UV-visible spectra of P3HT doped with acetic acid at 30×10^3 equivalents 30 min after the addition.

3.3.4 Doping with chloroacetic acid (CA), dichloroacetic acid (DCA) and trichloroacetic acid (TCA)

The solid CA and TCA were first dissolved in CHCl_3 and added into P3HT solution while DCA was added directly as a liquid. The calculated AC-index values are shown in Figure 3.15.

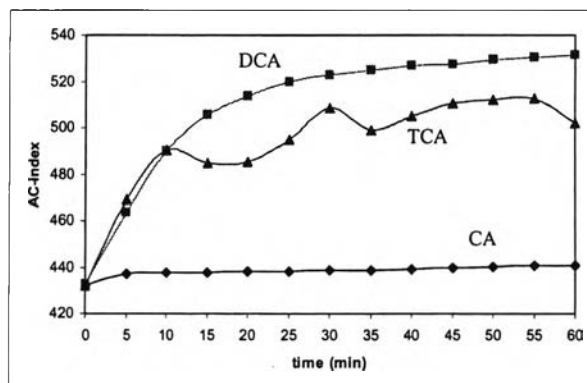


Figure 3.15 AC-index values of 0.3 μmol P3HT doped with acids at 3.33×10^3 equivalents during 60 min after additions (Table D-7, Appendix D).

The result showed a strange order of the extent of doping that did not correspond to the strength of the acids. When the experiments were repeated with doping directly by solid CA and TCA, the expected order of doping effect as a function of acid strength was observed as shown in Figure 3.16.

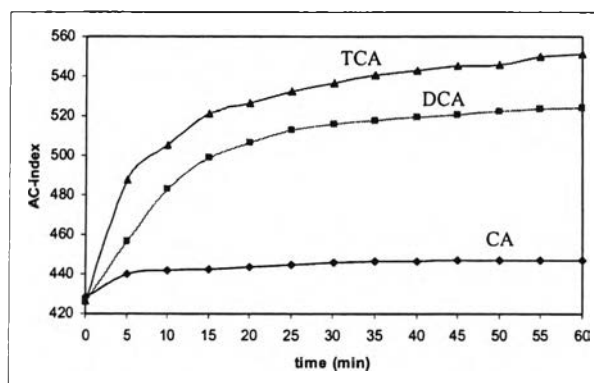


Figure 3.16 AC-index values of 0.3 μmol P3HT doped with acids at 3.33×10^3 equivalents during 60 min after additions (Table D-8, Appendix D).

This result showed that CA ($\text{pK}_a = 2.87$) [49] is too weak to dope P3HT which was similar to acetic acid ($\text{pK}_a = 4.76$). The stronger DCA ($\text{pK}_a = 1.35$) and TCA ($\text{pK}_a = 0.66$) could dope P3HT, although it took a long time to stabilize and reach the equilibrium. The problem of presolvation in CHCl_3 on reducing the doping strength was confirmed by an experiment using DCA predissolved in CHCl_3 as the doping agent. As expected, the lower AC-index values at equilibrium was observed as shown in Figure 3.17.

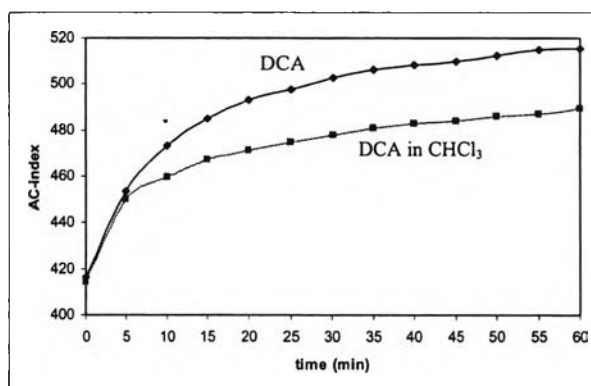


Figure 3.17 AC-index values of $0.3 \mu\text{mol}$ P3HT doped with acid at 3.33×10^3 equivalents during 60 min after additions (Table D-9, Appendix D).

The lowering effect on doping strength from such relatively inert solvent as CHCl_3 was peculiar at first. We postulated that perhaps the moisture absorbed into the solution during the highly humid weather might be responsible for the effect. To prove this assumption, we doped $0.6 \mu\text{mol}$ P3HT with 6.67×10^3 equivalents of TCA and then separated the solution into 2 batches. The first batch followed the normal procedure while the second batch was added $10 \mu\text{L}$ water before monitoring by UV-visible spectroscopy. Furthermore, CHCl_3 was dried by molecular sieves and used to dissolve TCA before adding into P3HT solution. The results from these 3 conditions were compared in Figure 3.18. The results confirmed that small moisture content in CHCl_3 did decrease the doping level of acid on P3HT.

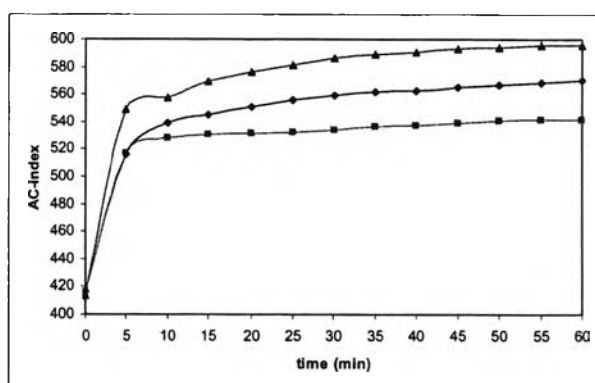


Figure 3.18 AC-index values of $0.3 \mu\text{mol}$ P3HT doped with acids at 3.33×10^3 equivalents during 60 min after additions: (◆) solid TCA; (■) solid TCA+H₂O; (▲) TCA in dry CHCl_3 (Table D-10, Appendix D).

The study of the doping level was carried out CA, DCA, and TCA were added in varied volume and the solutions were monitored at 839 nm where the polaron was presumed to absorb, (Figure 3.19) and compared with the corresponding AC-index values (Figure 3.20).

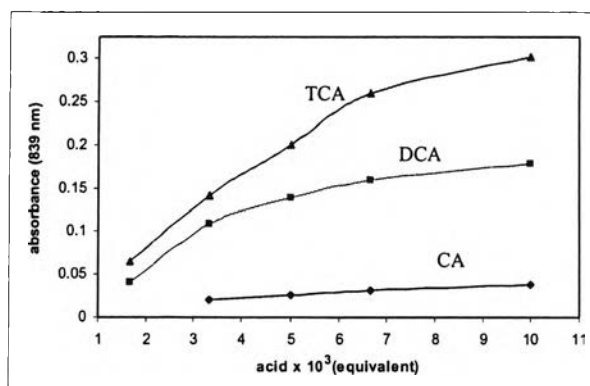


Figure 3.19 Absorbance at 839 nm of 0.3 μmol P3HT doped with acids : (◆) CA; (■) DCA; (▲) TCA (Table D-11, Appendix D).

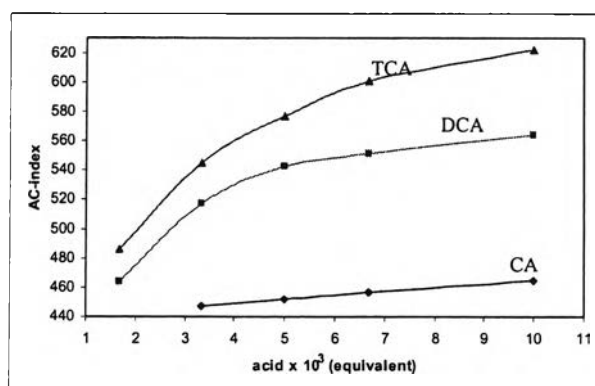


Figure 3.20 AC-index values of 0.3 μmol P3HT doped with acids : (◆) CA; (■) DCA; (▲) TCA (Table D-12, Appendix D).

Both results showed an almost parallel relation between either the absorbances or AC-index values to the addition of acid doping agent, indicating the potential of AC-index values to be used as an alternative tool to monitor the doping process.

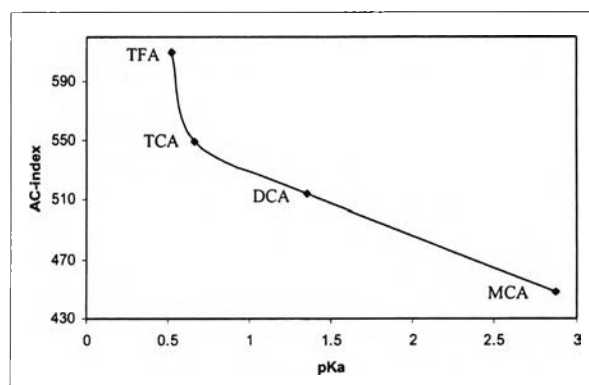


Figure 3.21 AC-index values of 0.3 μmol P3HT doped with 3.33×10^3 equivalents of acids ranged in their pK_a values (Table D-13, Appendix D).

When we plot the AC-index values of 0.3 μmol P3HT doped with 3.33×10^3 equivalents of CA, DCA, TCA, and TFA, it was found that the AC-index values of chloroacetic acid derivative-doping increased linearly with the acidity of the acids. However, TFA which is only slightly more acidic than TCA gave unusually higher AC-index value than TCA. The possible explanation may be due to the involvement of the counter anion in the doping process in which, the smaller trifluoroacetate may better facilitate the doping of polymer.

3.3.5 Doping with toluene-4-sulfonic acid

The problem of water content was also encountered in the doping of poly(3-hexylthiophene) with toluene-4-sulfonic acid monohydrate ($\text{TsOH} \cdot \text{H}_2\text{O}$). The doping level of $\text{TsOH} \cdot \text{H}_2\text{O}$ was comparable to TFA despite its lower pK_a ($\text{pK}_a = -1.34$) [49] (Figure 3.22). After removing water from the monohydrate form of TsOH, an obvious increase of AC-index values was observed.

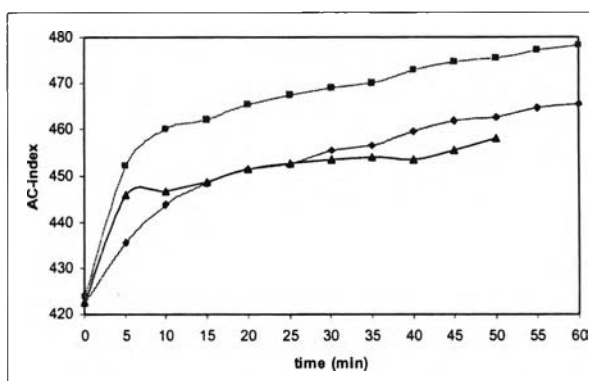


Figure 3.22 AC-index values of P3HT doped with acids at 0.83×10^3 equivalents :
 (◆) TsOH.H₂O; (■) TsOH; (▲) anhydrous TFA (Table D-14, Appendix D)

3.4 The doping of P3HT fraction with TFA

Each fraction of P3HT was doped with TFA according to Table 2.1 and the λ_{\max} and AC-index values were obtained from UV-visible spectra. The starting AC-index values of the undoped fractions were adjusted to make them close together in order to facilitate the comparison of their doping progress. The plot of AC-index values against of added TFA is shown in Figure 3.23.

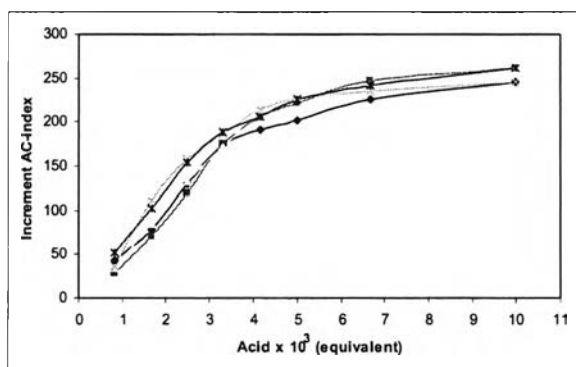


Figure 3.23 Increase of AC-index values of poly(3-hexylthiophene) fractions upon doping with Trifluoroacetic acid (TFA): (◆) acetone ; (■) hexane ; (▲) CH₂Cl₂ ; (×) 10%CHCl₃ in CH₂Cl₂ ; (*) CHCl₃ (Table D-15, Appendix D).

From the result in Figure 3.23, AC-index values of all fractions similarly increase with added TFA until almost reaching saturation at about $5.00 - 6.67 \times 10^3$

equivalents of acid when the curve reach the equilibrium. Moreover, when compare their results together, we found that all of them have the similar trend of AC-index curve. It implies that structure and size of each P3HT fraction have almost no contribution to their doping behavior.

3.5 Oxidation of P3HT

3.5.1 By H₂O₂/TFA

For all oxidations with acid catalyst, the acid reagent could act as doping agent and obscure the results from real oxidations in the UV-visible spectra analysis. Consequently, all products were washed with 0.1 M NaOH before UV-visible measurement.

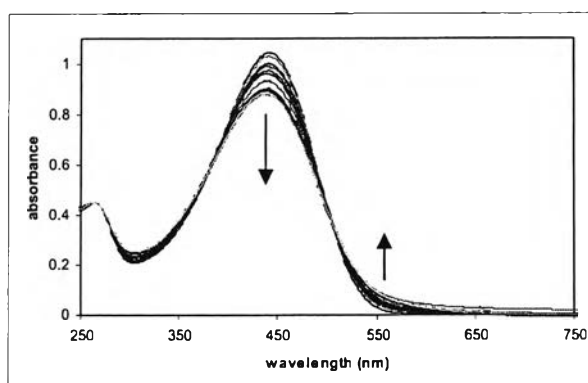


Figure 3.24 UV-visible spectra of P3HT oxidized by H₂O₂/TFA from 10 to 120 min oxidation. Arrows indicate the directions of absorbance changes of that areas over time.

As the reaction continued, there was a reduction of the absorbance at 441 nm (λ_{max}) with the slight increase of the absorbance at higher wavelengths (**Figure 3.24**). This increase of the absorbance seemed to level off after longer oxidation times (beyond 120 min) while the absorbance at 441 nm continued to decline. This was presumably due to the continued degradation of the polymer at the expense of the forming sulfone moieties initially generated from S-atom oxidation. It is assumed that the polymer chain had been degraded because of the overoxidation. This overoxidized degradation stemmed from the fact that the formation of sulfone group destroyed the aromaticity of the thiophene ring to give the prominent diene feature. Normally,

double bond would be oxidized more easily and could eventually be cleaved resulting in the chain scission. Low temperature could reduce the rate of the oxidative cleavage but would retard the S-atom oxidation as well. The degradation of polymer chain would yield the shortened polymer that lacked the desired conductive property.

The AC-index values calculated from the change in UV-visible spectra of P3HT oxidation are shown in **Figure 3.25**.

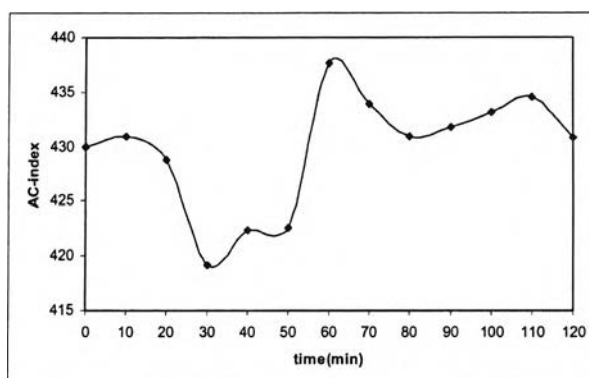


Figure 3.25 AC-index values of P3HT oxidized by $\text{H}_2\text{O}_2/\text{TFA}$ (mole ratio P3HT : H_2O_2 : TFA = 0.15 : 37.5 : 3.72) (**Table D-16**, Appendix D)

The oxidation by heterogeneous $\text{H}_2\text{O}_2/\text{TFA}$ was difficult to control and a good reproducibility was hard to obtain due to perhaps the limited contact of starting materials and the uneven distribution among phases. Because of the separation of H_2O_2 and P3HT in different phases, H_2O_2 was presumed to oxidize TFA to trifluoroperacetic acid which was then diffused into the organic phase to oxidize P3HT, producing sulfone and regenerating TFA, which then moved back to the aqueous phase to be oxidized by H_2O_2 and continued the cycle. The highly variable amount of trifluoroperacetic acid generated and moved between phases together with the highly volatility of many species would possibly be the reason for the disorder of the data obtained.

3.5.2 By Urea Hydrogen Peroxide (UHP)/TFA

The use of UHP in place of H_2O_2 was to avoid the volatility of the oxidizing agent and increase reproducibility. However, UHP is insoluble in CHCl_3 and the reactions perhaps went through the preoxidized TFA into peroxide, similar to H_2O_2 oxidation.

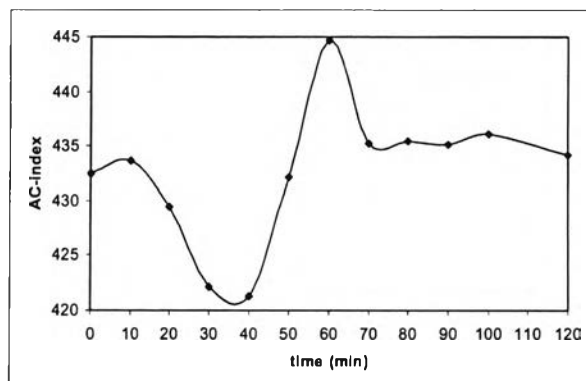


Figure 3.26 AC-index value of P3HT oxidized by UHP/TFA (mole ratio P3HT : UHP : TFA = 0.15 : 37.5 : 3.72) (Table D-17, Appendix D)

As a result, the same irreproducibility of the reactions were still obtained, which were also possibly due to variations of the reaction time, similar to H₂O₂/TFA oxidation.

Next, preoxidation was carried out by mixing UHP and TFA until the mixture became homogeneous, then the solution was added to react with P3HT at 0 °C. the conditions of the reactions are compiled in Table 3.4.

Table 3.4 The mole ratios of P3HT : UHP : TFA in preoxidized conditions.

entry	P3HT (mmol)	UHP (mmol)	TFA (mmol)	Mole ratios	Temp (°C)
1	0.15	37.5	37.5	1 : 250 : 250	0
2	0.03	0.75	7.5	1 : 25 : 250	0
3	0.09	2.25	67.5	1 : 25 : 750	0
4	0.09	4.50	9.0	1 : 50 : 100	0
5	0.09	2.25	4.5	1 : 25 : 50	0
6	0.05	0.10	0.2	1 : 2 : 4	0
7	0.05	0.10	0.2	1 : 2 : 4	55

At high concentration of oxidizing agent (entry 1, **Table 3.4**), the oxidized polymer immediately precipitated. To keep the solution homogeneous, P3HT was used (entry 2, **Table 3.4**). However, the reaction was very slow and remained fluctuating even after 4 hours. Although the similar trend to the H_2O_2 oxidation was found with the monitored UV-visible spectra (**Figure 3.27**).

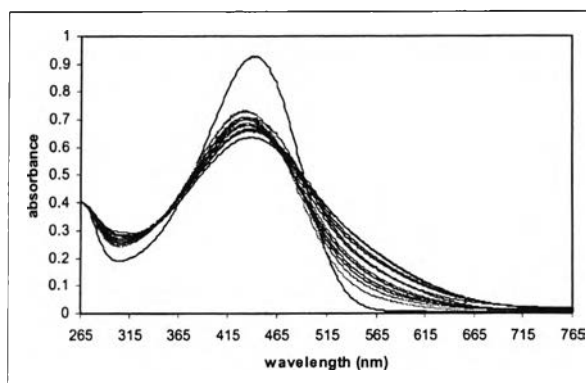


Figure 3.27 UV-visible spectra of P3HT was oxidized by UHP/TFA measuring every 10 min interval until 120 min (mole ratio P3HT : UHP : TFA = 0.03 : 0.75 : 7.5)

Increasing TFA to accelerate reaction instead resulted in the opposite direction in which little change was observed in the UV-visible spectra (entry 3, **Table 3.4** and **Figure 3.28**).

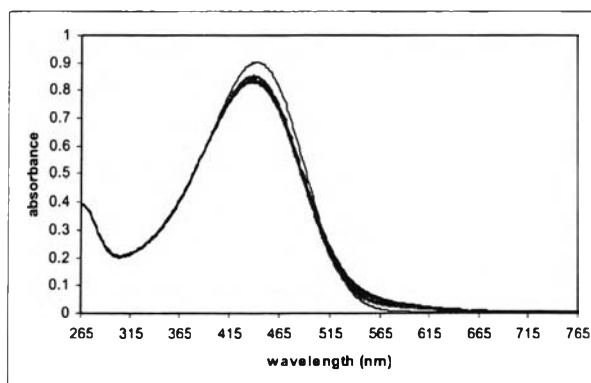


Figure 3.28 UV-visible spectra of P3HT was oxidized by UHP/TFA measuring every 10 min interval until 120 min (mole ratio P3HT : UHP : TFA = 0.09 : 2.25 : 67.5)

Raising the ratio of UHP at high concentration compared to P3HT yielded precipitation of oxidized polymer in various amounts (entries 4 and 5, **Table 3.4**). Finally, the oxidizing agent was kept at low ratios to maintain homogeneity (entry 6, **Table 3.4**) and the reaction temperature was raised to increase the reaction rate to the convenient level to be monitored by UV-visible spectroscopy (entry 7, **Table 3.4**). The calculated AC-index values are shown in **Figure 3.29**.

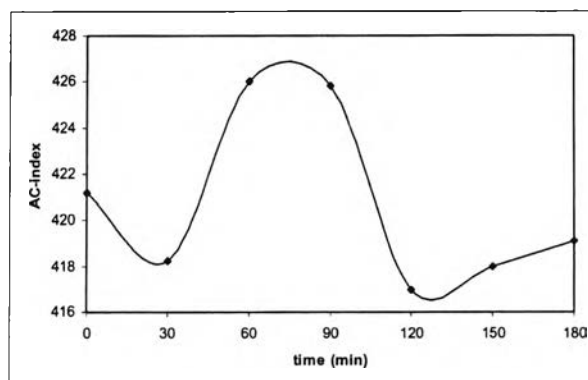


Figure 3.29 AC-index values of P3HT oxidized by UHP/TFA at 55 °C (mole ratio P3HT : UHP : TFA = 0.05 : 0.10 : 0.20) (**Table D-18**, Appendix D)

From **Figure 3.29**, AC-index value reached maximum at approximately 60 min of oxidation and started to fall after 90 min. This rather slow doping process may arise from the sluggish reorganization of the oxidized polymer in the solvent to achieve better conjugation of the π system that is slower than doping with protonic acid. Furthermore, the oxidized polymer could also be easily degraded by excess oxidizing agent resulting in lower AC-index values at longer reaction time and eventual precipitation of the too polar degraded fragments.

3.6 Solvato-controlled doping

Solvato-controlled doping [44] developed the new chemistry in which conducting polymers can be made soluble, spin-cast and formed solid film in a single step. The doping agent can be switched between non-oxidizing and oxidizing in the presence or absence of a coordinating ligand (or base). Removal of the coordinating ligand during thin-film processing should enable the oxidizing agent (or acid) to dope the polymer. In the current investigation, solutions containing P3HT and acid, which usually undergo spontaneous reactions, doping, and precipitation, were presumed to

be stabilized using selected types of coordinating ligands or bases. Upon removal of the coordinating ligand, spontaneous oxidative doping of the polymer occurred. Uniform electronically conducting films were thus expected from such simultaneous evaporation of both solvent and coordinating ligand. **Table 3.5** showed the conditions used in various types of acid doping agents, coordinating bases and their mole ratios to the polymer.

Table 3.5 The mole ratios of P3HT : Acid : Base in solvato-controlled doping condition

Entry	Acid	Base	Mole ratios
			P3HT : Acid : Base
1	TsOH	H ₂ O	1 : 1 : 1
2	MSA	pyridine	1 : 1 : 2
3	MSA	Triethylamine	1 : 1 : 2
4	DCA	Triethylamine	1 : 1 : 2
5	DCA	Thiophene	1 : 2 : 4
6	DCA	Thiophene	1 : 0.5 : 0.5
7	MSA	Thiophene	1 : 0.5 : 1
8	MSA	Triethylamine	1 : 0.5 : 1

We started out with TsOH as a doping agent. The water in the crystal functioning as the base or coordinating ligand (entry 1, **Table 3.5**). Upon evaporation we found the acid recrystallized on the surface of the polymer film and resulted in a raise of the baseline absorption of the UV-visible spectrum and covered all absorption of the analyte that might have appeared. Next, MSA was used because of its high acidity and boiling point, and pyridine was used as the base or coordinating ligand (entry 2, **Table 3.5**). When the mixture of MSA and pyridine was added to the reaction, the pyridinium salt precipitated out of CHCl₃. The film cast from this mixture showed high baseline absorption in UV-visible spectrum. The pyridinium salt was not or only slightly volatile and the ligand could not be removed from the film.

The polymer remained partly undoped, indicating the unsuccessful solvato-controlled doping in this condition. The result is shown in **Figure 3.30**.

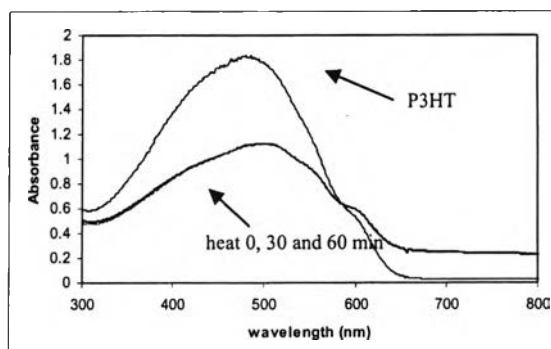


Figure 3.30 UV-visible spectra of P3HT, which was solvato-controlled doped by MSA and pyridine, measuring after heating at 80 °C for 0, 30 and 60 min (mole ratio P3HT : MSA : pyridine = 1 : 1 : 2)

The base was changed from pyridine to triethylamine to enhance the solubility in CHCl_3 and be more easily removed due to the lower boiling point (70 °C) (entry 3, **Table 3.5** and **Figure 3.31**). Orange homogeneous solution was obtained at first but immediate precipitation occurred upon casting film. The UV-visible spectra showed high baseline even after heating to 80 °C. The polymer may have been degraded in to the final mixture of opaque salt and dark precipitation.

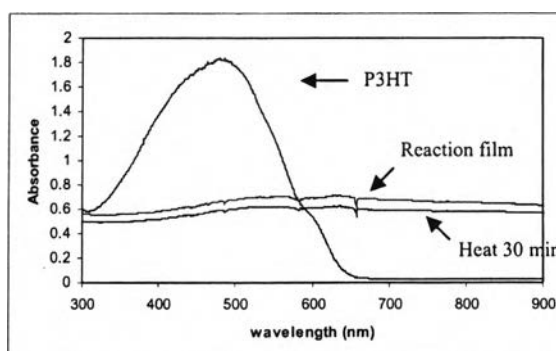


Figure 3.31 UV-visible spectra of P3HT which was solvato-controlled doped by MSA and triethylamine, measuring after heating at 80 °C for 0, 30 min (mole ratio P3HT : MSA : triethylamine = 1 : 1 : 2).

Changing MSA to DCA (entry 4, **Table 3.5**) to lower the acidity gave smooth doped P3HT film but the baseline of UV-visible spectrum was still high.

When the film was heated, the doped polymer also degraded. These repeated problems suggested that triethylamine was not appropriate as a base in solvato-controlled doping. Consequently, we replaced triethylamine with thiophene because of its similarity to P3HT and the possibility to prevent intramolecular interactions that led to precipitation of the doped polymer (entry 5 and 6, **Table 3.5**). We obtained homogeneous reaction, the film was smooth, and the baseline of the UV-visible spectrum rised up slightly that could be minimized by lowering acid and base.

The use of MSA was resumed because of its higher acidity and boiling point. Smooth film and increased doping rate were obtained with increased time of heating (entry 7, **Table 3.5**, **Figures 3.32** and **3.33**).

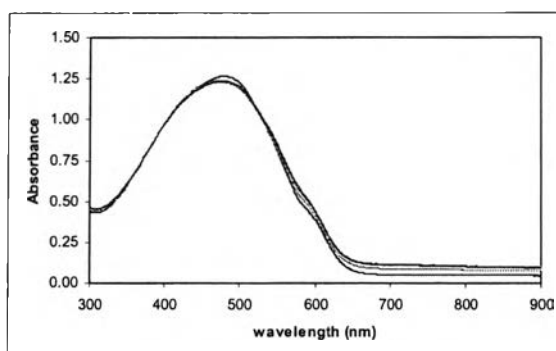


Figure 3.32 UV-visible spectra of P3HT which was solvato-controlled doped by MSA and thiophene, measuring after heating at 60 °C every 10 min interval until 100 min (mole ratio P3HT : MSA : thiophene = 1 : 0.5 : 1).

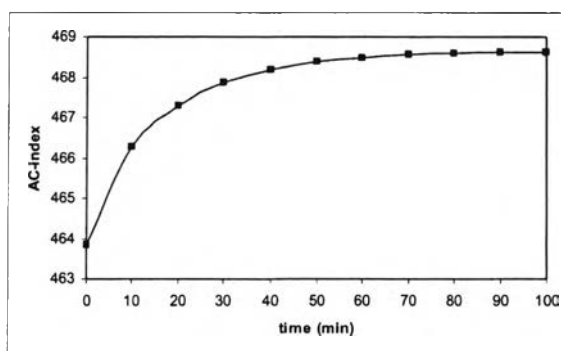


Figure 3.33 AC-index values of P3HT which was solvato-controlled doped by MSA and thiophene (mole ratio P3HT : MSA : thiophene = 1 : 0.5 : 1) (**Table D-19**, Appendix D).

From **Figure 3.33**, it was shown that AC-index values increased until 60 min after casting film. Successful solvato-controlled doping may have been obtained.

3.7 Conductivity measurement

3.7.1 Polymer Solution by conductometer

Result of the measured conductivity of acid-doped polymer by conductometric method at concentration ratios of polymer to acid according to **Table 2.2** are showed in **Figure 3.34**.

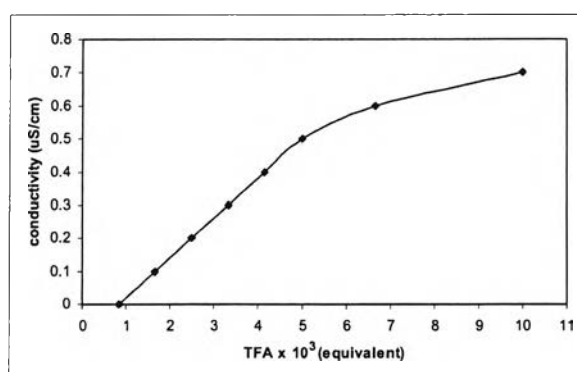


Figure 3.34 Conductivity of 0.45 mM P3HT doped by TFA (**Table D-20**, Appendix D).

From **Figure 3.34**, the conductivity curve is quite similar to AC-index curve obtained at comparable equivalent of TFA doping, albeit at different concentration (**Figure 3.12**). Both optical (from AC-index) and electrical (conductivity) properties seemed to level off at approximately $5-6 \times 10^3$ equivalents of TFA doping, supporting the possible correlation of the two analytical methods and properties that both perhaps arised from the alteration of the conjugation in polymer structure.

In the experiment, 0.45-16.67 M P3HT were doped with TFA according to **Table 2.2** giving the results shown in **Figure 3.12**. It was shown that the conductivity increased with the increasing concentration of polymer. This supports the expectation that the higher concentration of the doped polymer, which behaved as the electron transport, the higher conductivity of the solution.

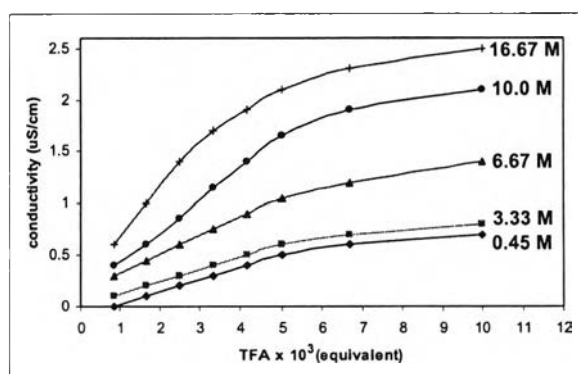


Figure 3.35 AC-index values of P3HT in various concentrations (Table D-21, Appendix D)

When the conductivity of the P3HT solutions that have been consecutively extracted into fraction of acetone, hexane, CH_2Cl_2 , 10% CHCl_3 in CH_2Cl_2 , and CHCl_3 fractions were measured, the results are shown in Figure 3.36. The acetone and hexane fractions gave high and almost equal conductivity, probably because they contained mostly the polymer molecules with lower molecular weights. At the same concentration of thienyl unit equivalence as used in the experiment, the acetone and hexane fractions would have more amount of polymer chains per unit volume, corresponding to higher concentration of electron transport molecules and hence increase the conductivity.

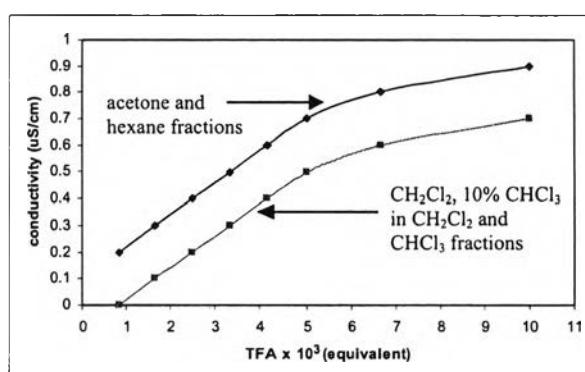


Figure 3.36 Conductivity of 0.05 mM P3HT fractions (Table D-22, Appendix D).

However, the unexpected separation of the conductivity curves of these 5 fractions into 2 groups rather than gradual decrease of conductivity following their average molecular weight remained unclear.

3.7.2 Polymer film by 4-Point Probe

3.7.2.1 P3HT film doped by iodine vapor

The conductive polymer doped by I₂ vapor is a popular method because it's easy to dope. But this method can dope the polymer only on the surface. The doping agent will slowly evaporate away with the gradual decrease of the conductivity of the polymer. In our experiment, we found that the I₂ doped polymer could not retain the constant conductive property when being taken out of I₂ chamber, as shown in **Table 3.6**.

Table 3.6 The decrease of conductivity of I₂ doped P3HT film after taken out of I₂ chamber.

Entry	Sample	Keep out of chamber (hr)	Thickness (μm)	Conductivity (S/cm)
1	P3HT film	-	10	7.25×10^{-7}
2 [11]	random P3HT film doped with I ₂	N/A	N/A	10
3 [11]	regular P3HT film doped with I ₂	N/A	N/A	1,350
4	P3HT film doped with I ₂ for 24 hr	4	10	5,190
5	P3HT film doped with I ₂ for 24 hr	5	10	2,160
6	P3HT film doped with I ₂ for 24 hr	6	10	1,920
7	P3HT film doped with I ₂ for 24 hr	7	10	423

N/A = information not available from Ref. 11

3.7.2.2 P3HT film doped by TCA

TCA was used because of its high boiling point and the doping solution are homogeneous. The acid doping is a more stable method than I₂ doping because it is not a surface doping. The results shown that the conductivity of the doped P3HT film increased with the higher amount of acid (**Table 3.7**).

Table 3.7 Conductivity of P3HT doped by TCA^a.

Entry	TCA (μmol)	Thickness (μm)	Conductivity (S/cm)
1	30	26	237
2	60	50	345
3	120	70	411
4	240	40	1,862

^a120 μmol of P3HT was used. See section 2.9.2

In entry 4, the as-synthesized P3HT could be heavily doped to give higher conductivity than even the regioregular HT-P3HT which was doped with I_2 (1,350 S/cm) [11]. This indicated that the acid doping could potentially be more efficient than the I_2 doping for P3HT.